JOURNAL OF BACTERIOLOGY, Jan. 2001, p. 700–708 Vol. 183, No. 2
0021-9193/01/$04.00+0 DOI: 10.1128/JB.183.2.700–708.2001

nag Genes of *Ralstonia* (Formerly *Pseudomonas*) sp. Strain U2 Encoding Enzymes for Gentisate Catabolism

NING-YI ZHOU, SERGIO L. FUENMAYOR,† AND PETER A. WILLIAMS*

School of Biological Sciences, University of Wales, Bangor, Gwynedd LL57 2UW, Wales, United Kingdom

Received 5 September 2000/Accepted 28 October 2000

Ralstonia **sp. strain U2 metabolizes naphthalene via gentisate to central metabolites. We have cloned and sequenced a 21.6-kb region spanning the *nag* genes. Upstream of the pathway genes are *nagY,* homologous to chemotaxis proteins, and *nagR,* a regulatory gene of the LysR family. Divergently transcribed from *nagR* are the genes for conversion of naphthalene to gentisate (*nagAaGHAbAcAdBFCQED*) (S. L. Fuenmayor, M. Wild, A. L. Boyes, and P. A. Williams, J. Bacteriol. 180:2522–2530, 1998), which except for the insertion of *nagGH*, encoding the salicylate 5-hydroxylase, are homologous to and in the same order as the genes in the classical upper pathway operon described for conversion of naphthalene to salicylate found in the NAH7 plasmid of *Pseudomonas putida* PpG7. Downstream of *nahD* is a cluster of genes (*nagJIKLMN*) which are probably co-transcribed with *nagAaGHAbAcAdBFCQED* as a single large operon. By cloning into expression vectors and by biochemical assays, three of these genes (*nagIKL*) have been shown to encode the enzymes involved in the further catabolism of gentisate to fumarate and pyruvate. NagI is a gentisate 1,2-dioxygenase which converts gentisate to maleylpyruvate and is also able to catalyze the oxidation of some substituted gentisates. NagL is a reduced glutathione-dependent maleylpyruvate isomerase catalyzing the isomerization of maleylpyruvate to fumarylpyruvate. NagK is a fumarylpyruvate hydrolase which hydrolyzes fumarylpyruvate to fumarate and pyruvate. The three other genes (*nagJMN*) have also been cloned and overexpressed, but no biochemical activities have been attributed to them. NagJ is homologous to a glutathione *S*-transferase, and NagM and NagN are proteins homologous to each other and to other proteins of unknown function. Downstream of the operon is a partial sequence with homology to a transposase.**

From the relatively low frequency of its appearance in the literature during the last 2 decades, the gentisate (2,5-dihydroxybenzoate) pathway in which a *p*-dihydroxylated aromatic ring is oxidatively cleaved might appear to be a less common route for bacterial aromatic catabolism than either of the more extensively studied pathways through catechols (*o*-dihydroxybenzenes). However, gentisate and substituted gentisates serve as key intermediates in the aerobic pathways for the metabolism of a large number of aromatic compounds, including 3-hydroxybenzoate (15, 24), substituted phenols (8, 23, 39), salicylate (37, 40), 3,6-dichloro-2-methoxybenzoate (53), and naphthalene (14, 17, 34). Ring cleavage of gentisate is catalyzed by gentisate 1,2-dioxygenase (GDO; EC1.13.11.4) to form maleylpyruvate (26). The further conversion of maleylpyruvate to central metabolites has been reported to proceed either by direct hydrolysis to pyruvate and maleate (5, 22, 39) or by isomerization to fumarylpyruvate and subsequent hydrolysis to fumarate and pyruvate (5, 8, 24, 27, 41, 49).

GDO has been purified from a number of organisms (7, 10, 13, 20, 53), partial N-terminal amino acid sequences have been determined for six (10, 13, 20, 53), and one has been subjected to mechanistic studies (19). However, the first nucleotide sequences for a GDO gene have appeared in the databanks only very recently: *nagI* in the catabolism of naphthalene by *Ralstonia* sp. strain U2 (accession number AF036940), *gtdA* in the catabolism of 3,6-dichloro-2-methoxybenzoate from *Sphingomonas* sp. strain RW5 (AJ224977), an unnamed gene in the catabolism of 3-phenylpropionate from the extreme halophile *Haloferax* sp. strain D1227 (AF069949), and *xlnE* in the xylenol-degrading *Pseudomonas alcaligenes* P25X (AF173167). The GDO genes from *Sphingomonas* sp. strain RW5 and from *Haloferax* sp. strain D1227 have been expressed and partially characterized (13, 53). However, the genetic determinants of the further catabolism of maleylpyruvate have not yet been described, although DNA encoding maleylpyruvate isomerase and fumarylpyruvate hydrolase activities has been cloned from both *Klebsiella pneumoniae* (41) and *Pseudomonas putida* (23) but without any nucleotide sequence information.

Ralstonia sp. strain U2 (originally classified as a *Pseudomonas* sp.) converts naphthalene to central metabolites via gentisate. A 5.7-kb region encoding both naphthalene dioxygenase (*nagAaAbAcAd*) and salicylate 5-hydroxylase (*nagGH*) has previously been sequenced and functionally analyzed, revealing a novel gene order of *nagAaGHAbAcAd* (14). In this paper, we report the cloning and sequencing of overlapping fragments from strain U2 covering a continuous 21.6 kb of the *nag* genes and the characterization of genes encoding the enzymes involved in catabolism to central metabolites of gentisate formed from naphthalene.

MATERIALS AND METHODS

Bacterial plasmids and strains. The bacterial plasmids used and constructed in this study are listed in Table 1. *Escherichia coli* DH5α [ϕ80d*lacZ*ΔM15 *recA1 endA1 gyrA96 thi-1 hsdR17*(r_K^- m_K^+) *supE44 relA1 deoR* Δ(*lacZYA-argF*)*U169*] (Life Technologies, Paisley, United Kingdom) was used routinely as a host in cloning experiments. *E. coli* BL21(DE3)pLysS [F^- *ompT hsdS*$_B$(r_B^- m_B^-) *dcm*

* Corresponding author. Mailing address: School of Biological Sciences, Memorial Building, University of Wales Bangor, Bangor, Gwynedd LL57 2UW, Wales, United Kingdom. Phone: (44) 1248 382363. Fax: (44) 1248 370731. E-mail: P.A.Williams@bangor.ac.uk.

†Present address: Centro de Biotecnología, Instituto de Estudios Avanzados, Caracas 1015-A, Venezuela.

TABLE 1. Plasmids used and constructed in this study

Plasmid	Description	Source or reference
pUC18	Vector: Ap^r; multiple cloning site in *lacZ*α	57
pUC19	Vector: Ap^r; multiple cloning site in *lacZ*α	57
pET5a	Expression vector: Ap^r; *Nde*I site overlapping the initiating start codon downstream of T7 promoter and multicloning site	48
pGEM-T Easy	Vector: Ap^r; for cloning *Taq* polymerase-synthesized PCR fragment	Promega
pWWF6	8.5-kb *Bam*HI fragment from strain U2 inserted into pUC18	14
pWWF19	7.6-kb *Bgl*II fragment from strain U2 inserted into pUC18	This study
pWWF24	8.3-kb *Xho*I fragment from strain U2 carrying the naphthalene dioxygenase region cloned in the *Xho*I site of pBluescript II SK(+/−)	14
pWWF60	8.9-kb *Eco*RI fragment from strain U2 inserted into pUC18	This study
pWWF41	PCR fragment containing *nagJ* inserted into pUC18	This study
pWWF51	851-bp *Nde*I-*Eco*RI-cut PCR fragment containing *nagJ* inserted into pET5a	This study
pWWF19-24	PCR fragment containing *nagI* inserted into pUC18	This study
pWWF19-25	1,286-bp *Nde*I-*Eco*RI-cut PCR fragment containing *nagI* inserted into pET5a	This study
pWWF42	PCR fragment containing *nagK* inserted into pUC18	This study
pWWF52	771-bp *Nde*I-*Eco*RI-cut PCR fragment containing *nagK* inserted into pET5a	This study
pWWF43	PCR fragment containing *nagL* inserted into pUC18	This study
pWWF53	739-bp *Nde*I-*Eco*RI-cut PCR fragment containing *nagL* inserted into pET5a	This study
pWWF61	PCR fragment containing *nagMN* inserted into pUC18	This study
pWWF71	2,087-bp *Nde*I-*Eco*RI-cut PCR fragment containing *nagMN* inserted into pET5a	This study
pWWF62	PCR fragment containing *nagM* inserted into pUC18	This study
pWWF72	1,141-bp *Nde*I-*Eco*RI-cut PCR fragment containing *nagM* inserted into pET5a	This study
pWWF63	PCR fragment containing *nagN* inserted into pUC18	This study
pWWF73	1,222-bp *Nde*I-*Eco*RI-cut PCR fragment containing *nagN* inserted into pET5a	This study
pWWF80	6.5-kb *Hin*dIII fragment from pWWF60 subcloned into pUC18	This study
pWWF86	4.2-kb *Hin*dIII/*Sma*I fragment from pWWF80 subcloned into pUC19	This study
pWWF83	Deletion of the 3.8-kb *Sac*I fragment from pWWF80, containing *nagN*	This study
pWWF84	2.9-kb *Pvu*II/*Xho*I fragment containing *nagMN* from pWWF80 subcloned into pUC18	This study
pWWF96	0.8-kb *Msp*A1 I fragment containing *nagK* from pWWF86 subcloned into pUC18	This study
pWWF98	1.7-kb *Xmn*I/*Sal*I fragment containing *nagJ* from pWWF60 subcloned into pUC18	This study
pWWF100	3.3-kb *Hin*dIII/*Bgl*II fragment containing *nagIKL* from pWWF86 subcloned into pUC19	This study
pWWF105	pWWF100 with modified *Sgf*I site causing frameshift in *nagK*	This study

gal λ(DE3) pLysS (Cm^r)] (48) was purchased from Promega and used as the host for the overexpression of genes cloned in expression plasmid pET5a.

Media and bacterial culture. Liquid Luria-Bertani (LB) medium (32) containing the appropriate antibiotic was used for the cultivation of *E. coli* strains. Sensitivity test agar (LabM, Bury, United Kingdom) or LB agar were used with added ampicillin for the selection of strains carrying plasmids derived from pUC18, pET5a, or pGEM-TEasy. Minimal medium was prepared according to the description in reference 56. LB and minimal medium plates contained 1.5% agar (LabM). Cultures of strain U2 were grown on 10 mM Na succinate or 0.5% (wt/vol) naphthalene as a carbon source. The latter was added as powdered solid directly to liquid medium or spread on the lids of inverted petri dishes. Ampicillin was used at 100 μg/ml and kanamycin was used at 50 μg/ml where appropriate.

Plasmid extraction and DNA manipulation. Plasmid DNA was extracted from strain U2 by the method of Wheatcroft and Williams (54). Restriction endonuclease digestions and ligations with T4 ligase were done in accordance with the manufacturer's instructions. *E. coli* DH5α was transformed by standard procedures (42). Plasmids were purified by using the Concert Rapid Plasmid Mini System (Life Technologies).

Cloning of the 16S rRNA gene (rDNA) from *Ralstonia* sp. strain U2. The 27f and the 1492r universal primers (28) were used to amplify the 16S rDNA from strain U2 by PCR. The fragment generated was purified by agarose gel electrophoresis and band extraction before it was cloned into the pGEM-T vector.

Cloning of *Ralstonia* sp. strain U2 plasmid DNA. In order to isolate DNA overlapping the 3′ end of pWWF6 (Fig. 1), digested plasmid DNA from strain U2 was ligated into pUC18. Transformants were screened for expression of 1,2-dihydroxynaphthalene dioxygenase (NagC) activity by spraying with 3-methylcatechol and selecting colonies producing the yellow product 2-hydroxy-6-oxohepta-2,4-dienoate. pWWF19 with a 7.6-kb *Bgl*II insert (Fig. 1) was thus selected. To identify fragments overlapping the 3′ end of pWWF19 (Fig. 1), Southern hybridizations (46) using the ECL direct nucleic acid labeling and detection system (Amersham) were made against digests of plasmid DNA from U2. The probe was a 401-bp PCR-generated fragment (bases 16580 to 16980) obtained from pWWF19 by using two primers, 5′-TCGGCTTGACGAAAAAT ACG and 5′-GGATGCAGGCGTCAGCAGAA. The region of the gel that hybridized to the probe was excised, and its DNA was extracted and cloned into pUC18. Transformant colonies carrying DNA homologous to the probe were identified by colony hybridization, and pWWF60, carrying an 8.9-kb *Eco*RI insert, was finally selected (Fig. 1).

Expression of *nagJ*, *nagI*, *nagK*, *nagL*, *nagM*, and *nagN*. Pairs of oligonucleotide primers were designed to produce PCR fragments of each *nag* gene singly and *nagM* and *nagN* together. These were designed with (i) an *Nde*I site introduced at the putative ATG start codon of each reading frame, (ii) an *Eco*RI restriction site upstream of the *Nde*I site, and (iii) an *Eco*RI restriction site downstream of the gene. Initially the amplified fragment was cut at the two *Eco*RI sites and inserted first into pUC18. In this way, the *nagJ*, *nagI*, *nagK*, *nagL*, *nagMN*, *nagM*, and *nagN* genes were amplified from pWWF60 by using *Pfu* polymerase (Promega) to create pWWF41, pWWF19-24, pWWF42, pWWF43, pWWF61, pWWF62, and pWWF63, respectively (Table 1). The inserts of these clones were sequenced on a single strand to ensure that no mutation had been incorporated during the PCR. Fragments from each of these clones were then excised with *Nde*I and *Eco*RI, religated into the expression vector pET5a, and transformed into *E. coli* DH5α to produce plasmids pWWF51 (*nagJ*), pWWF19-25 (*nagI*), pWWF52 (*nagK*), pWWF53 (*nagL*), pWWF71 (*nagMN*), pWWF72 (*nagM*), and pWWF73 (*nagN*). All the pET5a constructs were subsequently transformed into *E. coli* BL21(DE3)pLysS. In the following list of the PCR primers used to make these plasmids, the *Nde*I site is italicized, the *Eco*RI site used for cloning into pUC18 is underlined, and the bases that differ from those in the wild-type sequence are in boldface: *nagJ* (forward), 5′-TTGATTTTAA**G**A**A**T**T**C***AT***ATG* AAGCTTTATTACAGC-3′; *nagJ* (reverse), 5′-GATACGCTC**G**A**A**TTCCATC AAGCATGTGGATAGG-3′; *nagI* (forward), 5′-AGC**G**A**A**T**T*****C*****AT***ATG*AGTC ACGAACTTGGCCG-3′; *nagI* (reverse), 5′-ACC**G**A**A**TTCCACCAGGGTTTG TGGCGATTT-3′; *nagK* (forward), 5′-ACGC**G**A**A**T**T**CGGTG***CATATG***GGCC GTCCG-3′; *nagK* (reverse), 5′-AGCGCGG**G**A**A**T**T**CACTGCTGTGGGTTCA G-3′; *nagL* (forward), 5′-TGAGCC**G**A**A**T**T*****C*****AT***ATG*AAGCTGTACAACTTCT GG-3′; *nagL* (reverse), 5′-CCTTAC**G**A**A**TTCACTATTGCTCATTGATACTT GTC-3′; *nagM* (forward), 5′-CAGTGA**G**A**A**T**T*****C*****ATATG***AGCAATAGTG-3′; *nagM* (reverse), 5′-CGGTTG**G**A**A**T**T**CGACGCTTCTTAC-3′; *nagN* (forward), 5′-GAGG**G**A**A**T**T*****C*****ATATG***ATCAAACGCC-3′; *nagN* (reverse), 5′-TAGCC**G** AATTCAACTGCGCCAGGT-3′; *nagMN* (forward), 5′-CAGTGA**G**A**A**T**T*****C*****A**

TABLE 2. *Ralstonia* sp. strain U2 genes and gene products

Gene designation	Putative function of gene product	Position in sequence	Product size (residues, kDa)	Most similar gene product(s) (species, % amino acid identity, accession no.) or reference
nagY (partial)	Chemotaxis protein	1–1272	422, 44.1 (partial 3′ end)	Chemoreceptor protein, Tar (*S. typhimurium*, 59, J01809)
nagR	Transcription activator	2144–1239	301, 33.8	Transcription activator, NahR (*P. putida* plasmid NAH7, 61, J04233)
nagAa	Ferredoxin reductase	2261–3247	328, 35.1	14
nagG	Salicylate-5-hydroxylase, large oxygenase component	3293–4564	423, 48.8	14
nagH	Salicylate-5-hydroxylase, small oxygenase component	4567–5052	161, 18.8	14
nagAb	Ferredoxin	5063–5377	104, 11.6	14
nagAc	Naphthalene dioxygenase, large oxygenase component	5464–6807	447, 49.6	14
nagAd	Naphthalene dioxygenase, small oxygenase component	6822–7406	194, 23.0	14
nagB	*cis*-Naphthalene dihydrodiol dehydrogenase	7470–8249	259, 27.1	*cis*-Naphthalene dihydrodiol dehydrogenase-like protein, PahB (*C. testosteroni* strain H, 98, AF252550)
nagF	Salicylaldehyde dehydrogenase	8298–9749	483, 51.9	Salicylaldehyde dehydrogenase, NahF (*P. putida* plasmid NPL1, 89, AF010471)
nagC	1,2-Dihydroxynaphthalene dioxygenase	9775–10683	302, 33.8	1,2-Dihydroxynaphthalene dioxygenase, NahC (*P. putida* plasmid NPL1, 88, AF010471)
nagQ	Putative aldolase	10753–11391	212, 22.8	Dibenzothiophene metabolism operon protein, DoxH (*Pseudomonas* sp. strain C18, 77, M60405)
nagE	*trans-o*-Hydroxybenzylidenepyruvate hydratase–aldolase	11449–12486	345, 38.2	*trans*-o-Hydroxybenzylidenepyruvate hydratase–aldolase, DoxI (*Pseudomonas* sp. strain C18, 88, M60405)
nagD	2-Hydroxychromene carboxylate isomerase	12669–13268	199, 23.1	2-Hydroxychromene-2-carboxylate dehydrogenase, NahD (*P. stutzeri*, 69, AF039533)
nagJ	GST homolog	13327–13932	201, 22.1	GST, BphK (*Pseudomonas* sp., 58, X76500)
nagI	GDO	14136–15203	355, 39.9	GDO, GdtA (*Sphingomonas* sp. strain RW5, 35, AJ224977); GDO, XlnE (*P. alcaligenes*, 34, AF173167)
nagK	Fumarylpyruvate hydrolase	15360–15938	192, 20.9	Unknown Orf2 (*Sphingomonas* sp. strain RW1, 56, Y13118); unknown Orf2 (*Sphiingomonas* sp. strain RW5, 51, AJ224977)
nagL	Maleylpyruvate isomerase	15950–16588	212, 23.5	Unknown Orf3 (*Sphingomonas* sp. strain RW1, 45, Y13118); maleylacetoacetate isomerase, MaiA (*S. meliloti*, 45, AF 109131)
nagM	Unknown	16651–17676	341, 35.5	NagN (39%) (this study); unknown Orf4 (*C. testosteroni* TA441, 31, AB024335); unknown Orf5 (*C. testosteroni* TA441, 31, AB024335)
nagN	Unknown	17693–18688	331, 34.9	NagM (39%) (this study); unknown Orf4 (*C. testosteroni* TA441, 31, AB024335); unknown Orf5 (*C. testosteroni* TA441, 30, AB024335)
orf1	Unknown	19375–19923	182, 18.9	No obvious homolog
tnpA (partial)	Transposase	20038–21159	374, 42.2 (partial 5′ end)	Transposase for IS1071 in transposon Tn*5271* (*Alcaligenes* sp. strain BR60, 99, M65135) (970 amino acids)

*TATG*AGCAATAGTG-3′; and *nagMN* (reverse), 5′-AAGTGGGCGAATTCA ACGAGAGGTTA′-3.

The Nag proteins encoded on the pET5a recombinants pWWF51 (*nagJ*), pWWF19-25 (*nagI*), pWWF52 (*nagK*), pWWF53 (*nagL*), pWWF71 (*nagM*), pWWF72 (*nagN*), and pWWF73 (*nagMN*) were individually expressed in *E. coli* BL21(DE3)pLysS by growth in LB medium at 37°C to an optical density at 600 nm of 0.6 and then induced for 4 h by addition of IPTG (isopropyl-β-D-thiogalactopyranoside). Sodium dodecyl sulfate-polyacrylamide gel electrophoresis (SDS-PAGE) was performed on a discontinuous gel in a Mini-PROTEIN II Electrophoresis Cell (Bio-Rad) according to the manufacturer's instructions. The Nag proteins encoded on the pUC18 recombinants pWWF83 (*nagN*), pWWF84 (*nagMN*), pWWF96 (*nagK*), and pWWF98 (*nagJ*) were also individually expressed in *E. coli* DH5α as described above.

Inactivation of *nagK*. pWWF100 was digested at its single *Sgf*I site within *nagK*. The 3′ overhangs of the *Sgf*I site were converted to blunt ends by 3′-to-5′ exonuclease action of T4 DNA polymerase (Promega), and the blunt ends were religated to produce pWWF105 (Fig. 1; Table 1.)

Preparation of cell extract. Cell extracts were prepared by resuspending the bacterial pellets in ice-cold 100 mM phosphate buffer (pH 7.4; approximately 0.1 g [wet weight]/ml) and disrupting them by sonication in an ice-water bath for three periods of 30 s with 30-s intervals, after which cell debris was removed by centrifugation at 100,000 × *g* for 1 h at 4°C.

Sequence determination and analysis. Nucleotide sequences were determined by MWG-Biotech Ltd. (Ebersberg, Germany). Sequences were analyzed with the Lasergene software package (DNASTAR). BLASTP was used for the deduced amino acid identity search, and BLASTN was used for the nucleotide sequence identity search (1). Pfam was used for the protein family search (4).

Enzyme assays. All assays were performed in 100 mM phosphate buffer (pH 7.4). GDO was assayed by measuring the increase in absorbance at 330 nm due to conversion of gentisate to maleylpyruvate (26), the molar extinction coefficient of which was taken as 13,000 M^{-1} cm^{-1} (26). GDO oxidation of substituted gentisates was assayed by measuring the increase in absorbance at 324 nm (for 3-methylgentisate), 334 nm (for 3-bromogentisate), and 324 nm (for 3-isopropylgentisate) due to their corresponding products (20): their molar extinction coefficients were taken as 13,500 M^{-1} cm^{-1}, 11,800 M^{-1} cm^{-1}, and 14,100 M^{-1} $cm^{-1,}$ respectively (20). The substituted gentisates were kindly supplied by C. L. Poh, National University of Singapore. Maleylpyruvate isomerase was qualitatively monitored by measuring the change in absorbance at 330 nm due to maleylpyruvate disappearance in the presence of glutathione (GSH). For quantitative determination of specific activity, the rate of change of A_{330} was measured in the presence of excess fumarylpyruvate hydrolase (NagK). Fumarylpyruvate hydrolase was assayed by measuring the decrease in A_{340} due to fumarylpyruvate disappearance: the molar extinction coefficient of fumarylpyruvate was taken as 9,400 M^{-1} cm^{-1} (49). Protein concentrations were

TABLE 3. Substrate specificity of NagI GDO

Substrate	K_m (μM)	Relative activity[a]
Gentisate	22.4	100
3-Methylgentisate	10.7	63
3-Bromogentisate	5.3	25
3-Isopropylgentisate	ND[b]	76

[a] Activity relative to that on gentisate (set at 100) measured at 100 μM for each substrate. The specific activity of the extract of *E. coli*(pWWF19-25) was 2.52 U/mg.
[b] ND, not determined.

determined by the biuret procedure. One unit of enzyme activity is defined as the amount required for the disappearance (or production) of 1 μmol of substrate (or product) per min at 30°C. Specific activities are expressed as units per milligram of protein.

Determination of kinetic parameters. To determine K_m values, initial velocities were measured at several nonsaturating concentrations of each compound. Preliminary experiments determined the approximate value of K_m, and the accurate rate determinations were then performed with 10 substrate concentrations spanning the approximate K_m value. Initial velocities were analyzed by the direct linear method using the program EnzPack, which calculates the most probable values for the kinetic parameters with their 68% confidence limits (55).

Analysis of fumarate and pyruvate production from fumarylpyruvate by fumarylpyruvate hydrolase using HPLC. The fumarylpyruvate hydrolase reaction was initiated by adding 160 μl of cell extract of *E. coli* DH5α(pWWF96 [*nagK*]) to 20 ml of 100 μM fumarylpyruvate in 100 mM phosphate buffer (pH 7.4), produced in situ from gentisate by NagI and NagL. Samples (1.8 ml) were withdrawn from the reaction mixture at regular intervals, and the enzyme reaction was stopped by adding H_2SO_4 to each to a final concentration of 50 mM. Fumarate and pyruvate in each sample were measured by high-performance liquid chromatography (HPLC) using a CECIL-1100 chromatograph (Cecil Instruments, Cambridge, United Kingdom). Two hundred microliters of each sample was injected on to an Aminex HPX-87H column (300 by 7.8 mm) (Bio-Rad) run at ambient temperature with 2.5 mM H_2SO_4 as the eluant at a flow rate of 0.6 ml/min. Detection was by UV at 210 nm. Fumarate and pyruvate concentrations were determined by reference to standards of known concentrations.

Analysis of pyruvate production from fumarylpyruvate by fumarylpyruvate hydrolase using LDH. The concentration of pyruvate was determined by measuring the decrease of absorbance at 340 nm due to NADH oxidation in the presence of excess lactic dehydrogenase (LDH). The sample cuvette (1 ml) contained the products from hydrolysis of fumarylpyruvate (or, in the standards, pyruvate alone) plus 0.16 μmol of NADH in 100 mM phosphate buffer (pH 7.4). The reference cell contained only buffer. The assay was initiated by adding 0.64 mg (0.54 U) of LDH from rabbit muscle (EC 1.1.1.27) (Sigma) to both cuvettes: 1 U of LDH reduces 1.0 μmol of pyruvate to lactate per min. The molar extinction coefficient for NADH at 340 nm was taken to be 6,220 M^{-1} cm^{-1}. The stoichiometry of the reaction was calculated from the change in A_{340} resulting from the total conversion of amounts of substrate varying from 10 to 100 nmol.

Nucleotide sequence accession numbers. The DNA sequence of 21,160 bp of the *nag* genes has been submitted to GenBank under accession number AF036940. The DNA sequence of the 16S rDNA has been submitted to GenBank under accession number AF301897.

RESULTS

Reclassification of strain U2. The almost complete 16S rDNA of strain U2 was cloned and sequenced. The gene from this strain exhibited the highest identity (98%) to the 16S rDNA from three strains of the genus *Ralstonia* (accession numbers AF067657 [38], AF085226 [50], and AF098288 [33]),

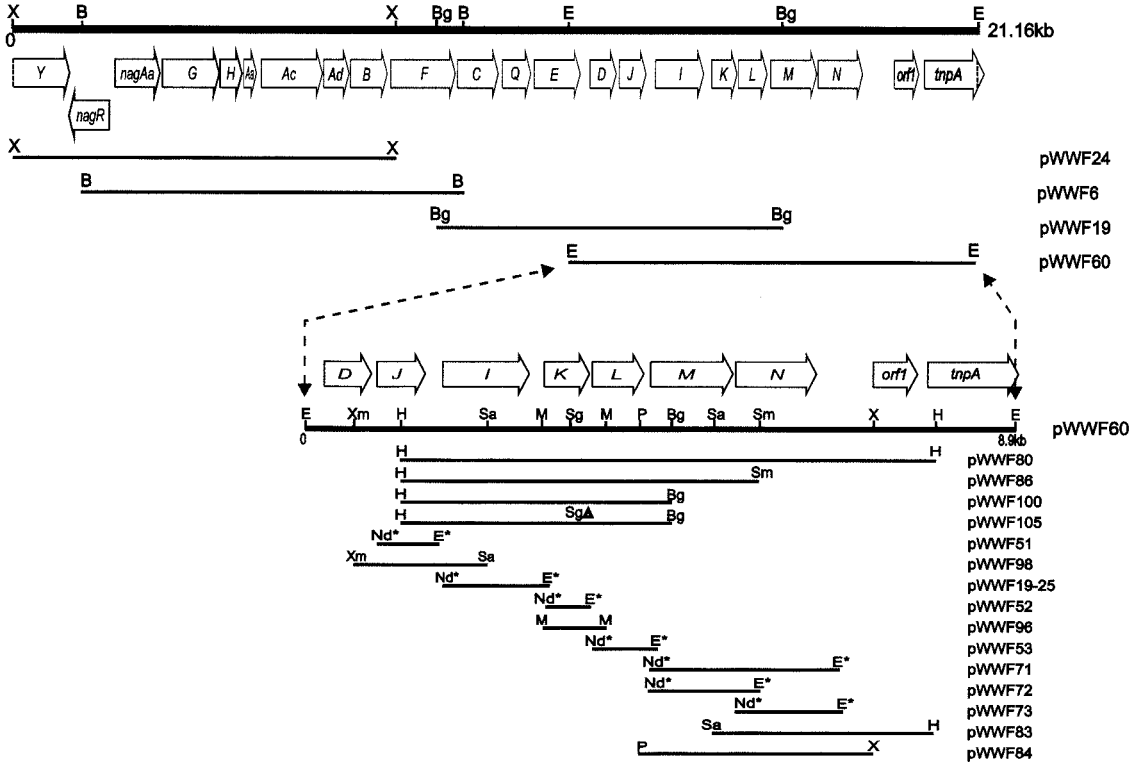

FIG. 1. Physical map of the *nag* gene cluster from the large catabolic plasmid of *Ralstonia* sp. strain U2 and inserts of recombinant plasmids constructed from it. ORFs are marked by the open arrows, with the direction of the arrowheads indicating the direction of transcription. The restriction sites are designated as follows: B, *Bam*HI; Bg, *Bgl*II; E, *Eco*RI; H, *Hin*dIII; M, *Msp*A1 I; P, *Pvu*II; Sa, *Sal*I; Sg, *Sgf*I; Sm, *Sma*I; X, *Xho*I. Nd* represents an *Nde*I site and E* represents an *Eco*RI site which were engineered in the PCR primer used to generate the inserts of pET5a constructs. SgΔ represents the modified *Sgf*I site causing a 2-bp deletion and a frameshift in *nagK*. Only restriction sites relevant to the clones and constructs indicated in this figure are shown.

indicating that it should be reclassified as *Ralstonia* sp. strain U2 rather than as a *Pseudomonas* sp.

Cloning of naphthalene catabolic genes. The genes for naphthalene dioxygenase (*nagAaAbAcAd*), together with those for the 5-salicylate hydroxylase (*nagGH*), naphthalene *cis*-dihydrodiol dehydrogenase (*nagB*), and salicylaldehyde dehydrogenase (*nagF*) were originally located on an 8.3-kb *Bam*HI fragment (pWWF6) with the novel gene order *nagAaGHAbAc AdBF* (14). With the important exception of the insertion of *nagGH* within the naphthalene dioxygenase cluster (*nagAaAb AcAd*), the gene order is identical to the *nahAaAbAcAdBF* found on the archetypal plasmid NAH7 (9, 45). We therefore hypothesized that the analogous *nagC* in U2 is downstream of *nagF* in pWWF6, as is the case in NAH7. Plasmid DNA of U2 was digested with *Bgl*II and ligated into *Bam*HI-digested vector pUC18. Transformants in *E. coli* DH5α were selected by screening for the yellow product (2-hydroxy-6-oxohepta-2,4-dienoate) produced from 3-methylcatechol (6) by 1,2-dihydroxynaphthalene dioxygenase (NagC). We identified a positive clone, designated pWWF19, that contained a 7.6-kb *Bgl*II insert. Sequence alignment confirmed its overlap with pWWF6 (Fig. 1). Further cloning of DNA downstream of pWWF19, as described in Materials and Methods, resulted in a plasmid, pWWF60, which contained an 8.9-kb *Eco*RI insert which overlapped with pWWF19 (Fig. 1).

Sequence analysis. Approximately 6 kb of DNA containing *nagAa* to *nagAd* of plasmid pWWF6 had been previously cloned and sequenced (14). Using pWWF6, pWWF19, pWW24, and pWWF60, sequencing was extended upstream of the 5′ end of *nagAa* and downstream of the 3′ end of *nagAd*, providing a continuous sequence of 21,160 bp, from which the presence of 20 complete open reading frames (ORFs) was deduced (Fig. 1; Table 2).

Upstream of *nagAa* is a divergently transcribed ORF (designated *nagR*). Its deduced amino acid sequence is very similar to that of the transcription activator NahR from *P. putida* plasmid NAH7 (44) and other regulatory proteins of the LysR family. Futher upstream is an incomplete ORF (designated *nagY*), but with a 34-bp overlap with *nagR*, the product of which was homologous to chemotaxis proteins from *Salmonella enterica* serovar Typhimurium and *E. coli* (35). Because of its location and its (admittedly low) similarity (30% amino acid identity) to the naphthalene chemotaxis protein from NAH7, NahY (16), we are making the tentative hypothesis that this is also a naphthalene chemotaxis protein.

Six complete ORFs (*nagBFCQED*) follow downstream of *nagAd*. The gene products all show strong similarity to those of the catabolic genes in the classical *nah* type operon (*nahBFC QED*) and are in the same order (Fig. 1; Table 2). We assume that they share the same functions as they have in plasmid NAH7, namely, the catabolic steps producing salicylate.

Unlike the classical *nah* operon, there are six further complete ORFs, *nagJ*, *nagI*, *nagK*, *nagL*, *nagM*, and *nagN*, found immediately after *nagD*, the homolog of the last gene (*nahD*) in the NAH7 upper pathway operon. These are transcribed in the same direction and, because of the small intergenic regions, are likely to be cotranscribed with the upstream *nag* genes. NagJ is similar to a group of glutathione *S*-transferases (GSTs) found in gene clusters involved in aromatic degradation (25, 30, 52), particularly to the GST homolog in the biphenyl-polychlorinated biphenyl degradation locus (*bph*) of *Pseudomonas* sp. strain LB400 (21). NagI is similar to GDOs from *P. alcaligenes* (10) and from *Sphingomonas* sp. strain RW5 (53). NagK corresponds to proteins of unknown function from two *Sphingomonas* strains, RW1 (3) and RW5 (53). NagL is a member of another subgroup of the GST superfamily and has greatest similarity to proteins of unknown function from the two *Sphingomonas* strains RW1 and RW5, the genes of both of which are also located downstream of NagK gene homologs (3, 53). After *nagL* there are two more ORFs, designated *nagM* and *nagN*. They are closer in sequence to each other than to the genes for any other proteins in the databases and are also similar to the genes for another pair of homologous proteins, Orf4 and Orf5, in a gene cluster encoding enzymes for the 3-(3-hydroxyphenyl) propionic acid degradation pathway from *Comamonas testosteroni* TA441 (2), both of which have been shown to be inessential for growth on 3-(3-hydroxyphenyl) propionic acid.

After *nagN* in plasmid pWWF60 there is a small ORF, designated *orf1*, which showed no homology to any sequence in the databases and, with an intergenic distance of 687 bp, is sufficiently far from *nagN* to be almost certainly part of a separate transcript. Further downstream are 374 codons of an incomplete ORF (designated *tnpA*) whose product is virtually identical (372 of 374 residues) to the transposase in IS1071, which is part of the chlorobenzoate catabolic transposon Tn*5271* from *Alcaligenes* sp. strain BR60 (36).

NagI catalyzes gentisate transformation. A PCR fragment containing the complete reading frame of *nagI* was ligated into expression vector pET5a as plasmid pWWF19-25 and transformed into *E. coli* BL21(DE3). After induction with IPTG, cell extracts were found to contain GDO with a specific activity of 2.52 U/mg against gentisate as the substrate. SDS-PAGE of the same extracts (data not shown) showed elevated levels of a polypeptide of ~40 kDa, as expected from the deduced amino acid composition. No activity or enhanced 40-kDa polypeptide band was detectable in controls where expression of the protein was not induced or where the expression vector contained no insert. Figure 2 shows the rapid transformation by the cell extract of gentisate (λ_{max} = 320 nm) to maleylpyruvate (λ_{max} = 330 nm) as described originally by Lack (26). GDO activity was also detected in the cell extract of strain U2 grown on naphthalene (0.078 U/mg). NagI exhibited an extended substrate specificity towards available alkyl and halogenated gentisates (Table 3). From these very limited data, K_m values for 3-substituted gentisates were found to be lower than those for gentisate, indicating a higher substrate affinity. However, the specific activities towards the substituted gentisates were also lower than towards gentisate, indicating a lower turnover number. A similar situation was reported for the GDOs in two *Pseudomonas* strains (10).

NagL catalyzes maleylpyruvate isomerization. pWWF53 carries the complete reading frame of *nagL* in expression vector pET5a (Table 1). When cell extracts of IPTG-induced *E. coli*(pWWF53) were incubated with maleylpyruvate, generated from gentisate by the action of NagI (as above), no change in the absorption spectrum between 250 and 400 nm took place unless GSH was introduced into the reaction. When GSH was present, the spectrum changed from a peak with a λ_{max} of 330 nm, characteristic of maleylpyruvate, to one with a λ_{max} of 340

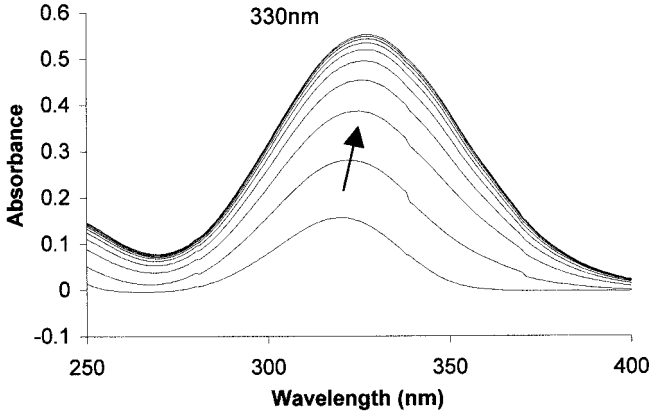

FIG. 2. Formation of maleylpyruvate from gentisate by cell extracts of *E. coli* DH5α(pWWF19-25 [*nagI*]) grown on LB medium containing 100 μg of ampicillin per ml, induced with 0.4 mM IPTG. Sample and reference cuvettes contained 100 mM phosphate buffer (pH 7.4) in 1-ml volumes. The sample cuvette also contained 0.05 μmol of gentisate. Spectra were recorded before and every 20 s after the addition of cell extract (5 μl containing 25 μg of protein). Cell extract was added to the reference cuvette in an equivalent amount.

nm and with a lower extinction coefficient (Fig. 3), as reported for that of fumarylpyruvate (26, 49). No equivalent reaction was seen in the presence of GSH without added cell extract or with added cell extract of *E. coli*(pET5a). We have noted that the change from maleylpyruvate to fumarylpyruvate occurs without a true isobestic point in the vicinity of 350 nm (Fig. 3), as has similarly been reported for the isomerization catalyzed by 4-oxalocrotonate tautomerase (29). This suggests that there might be a similar explanation, namely, that the reaction mechanism is more complex than just a direct interconversion of the two isomers. If the fumarylpyruvate was allowed to stand in the presence of excess GSH, then a slow change in spectrum

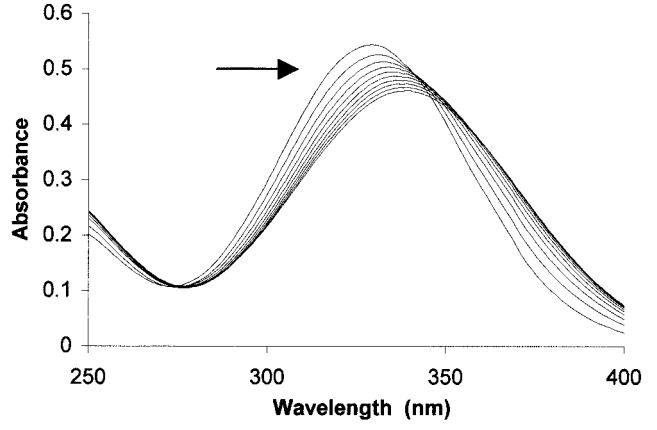

FIG. 3. Isomerization of maleylpyruvate to fumarylpyruvate by cell extracts of *E. coli* DH5α(pWWF53 [*nagL*]) grown on LB medium containing 100 μg of ampicillin per ml, induced with 0.4 mM IPTG. Sample and reference cuvettes contained 100 mM phosphate buffer (pH 7.4) and 1.0 μmol of reduced GSH in 1-ml volumes. The sample cuvette also contained maleylpyruvate transformed from 0.05 μmol of gentisate by gentisate dioxygenase (NagI) in situ. Spectra were recorded before and every 20 s after the addition of cell extract (5 μl containing 45 μg of protein). Cell extract was added to the reference cuvette in an equivalent amount.

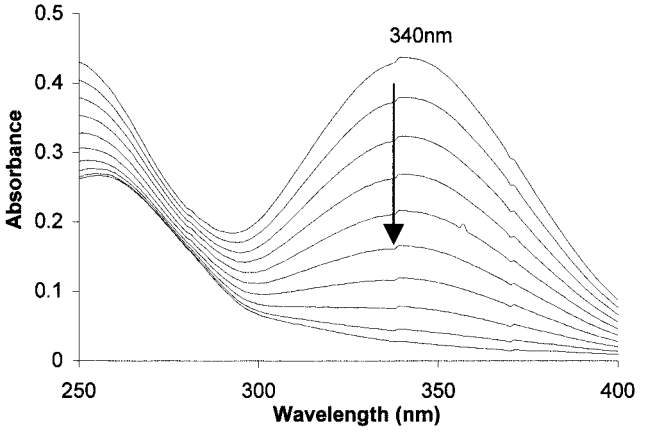

FIG. 4. Hydrolysis of fumarylpyruvate by cell extracts of *E. coli* DH5α (pWWF96 [*nagK*]) grown on LB medium containing 100 μg of ampicillin per ml, induced with 0.4 mM IPTG. Sample and reference cuvettes contained 100 mM phosphate buffer (pH 7.4) in 1-ml volumes. The sample cuvette also contained fumarylpyruvate formed from maleylpyruvate by the action of NagL (see the legend to Fig. 3), itself previously transformed from 0.05 μmol of gentisate by the gentisate dioxygenase (NagI) in situ. Spectra were recorded before and every 20 s after addition of cell extract (8 μl containing 90 μg of protein). Cell extract was added to the reference cuvette in an equivalent amount.

occurred, forming a product with a λ_{max} of 308 nm, as was described by Lack (27); this is assumed to be the result of a spontaneous nonenzymatic reaction between the two.

SDS-PAGE showed that induced cell extracts of *E. coli* (pWWF53) contained high levels of a polypeptide of ~23 kDa (data not shown), whereas no enhanced polypeptide band was detectable in controls where expression of the protein was not induced or where the expression vector contained no insert. The specific activity of maleylpyruvate isomerase was 1.23 U/mg in cell extracts of induced *E. coli* BL21(DE3) carrying pWWF53, and the same enzyme reaction was detected in a cell extract of strain U2 grown on naphthalene, but at a lower specific activity of 0.068U/mg.

NagK catalyzes fumarylpyruvate hydrolysis. Cell extracts of *E. coli*(pWWF52) carrying *nagK* inserted in pET5a (Table 1) showed no activity against fumarylpyruvate, formed from gentisate by the joint action of NagI and NagK, even though SDS-PAGE of induced cells showed a polypeptide of the right size (~21 kDa) expressed from this construct (data not shown); we assume that the high levels of expression produced an insoluble product in inclusion bodies. In order to reduce the expression, a 0.8-kb *Msp*A1 I fragment containing *nagK* was subcloned from pWW86 (Fig. 1; Table 1) into the *Hin*cII site of pUC18 in the correct orientation to the *lac* promoter, forming plasmid pWWF96. In contrast to the absence of activity in the pET5a-based construct, cell extracts of *E. coli*(pWW96) incubated with fumarylpyruvate effected the complete disappearance of the 340-nm peak (Fig. 4). The measured specific activity of fumarylpyruvate hydrolysis was 0.32 U/mg. The products of degradation from fumarylpyruvate were confirmed as pyruvate and fumarate by HPLC. Their retention times, under the conditions used, were 12 min 50 s and 22 min 30 s, respectively, and could be distinguished from those of other short-chain carboxylic acids, particularly maleate (retention time, 10 min 30 s). From the peak areas compared with those

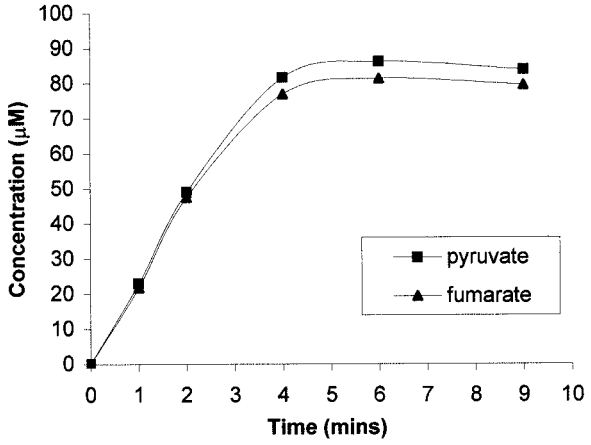

FIG. 5. Time course of production of fumarate and pyruvate from fumarylpyruvate by cell extracts of *E. coli* DH5α(pWWF96 [*nagK*]) grown on LB medium containing 100 μg of ampicillin per ml, induced with 0.4 mM IPTG. Reaction was initiated by adding 160 μl of cell extract to 20 ml of 100 μM fumarylpyruvate in 100 mM phosphate buffer (pH 7.4), produced in situ from gentisate by NagI and NagL. Fumarate and pyruvate were detected and quantified by HPLC on an Aminex HPX-87H column.

of standard amounts of the two products, it was calculated that equimolar amounts of pyruvate and fumarate were produced and that the stoichiometry of production of each was ultimately between 80 and 90% of the original gentisate added (Fig. 5). There was no maleate detected in the reaction. As additional confirmation that pyruvate was a product of fumarylpyruvate hydrolysis, NADH oxidation in the presence of LDH was used to measure pyruvate in the reaction mixture; 0.9 mol of NADH was oxidized per mol of fumarylpyruvate hydrolyzed, confirming the stoichiometry of pyruvate production. Fumarylpyruvate hydrolase activity was also detected in cell extracts of the U2 strain grown on naphthalene (0.075 U/mg).

Enzyme activities encoded on recombinant plasmids. By the enzyme assays for GDO, maleylpyruvate isomerase, and fumarylpyruvate hydrolase it was shown that all three activities could be detected in cell extracts of *E. coli* carrying any of the large cloned fragments on plasmids pWWF60, pWWF80, and pWWF86 and also on pWWF100, which carries only the three intact genes *nagIKL* (Fig. 1; Table 1). However, in *E. coli* carrying pWWF105, a derivative of pWWF100 with a frameshift within *nagK*, fumarylpyruvate hydrolase activity was not detected but both GDO and maleylpyruvate isomerase activities remained.

***nagJ*, *nagM*, and *nagN* appear to have no enzymatic role in gentisate metabolism.** The remaining genes, *nagJ*, *nagM*, and *nagN*, were also expressed from their insertions in both pET5a (pWWF51, pWWF71, pWWF72, and pWWF73 [Table 1]) and in pUC18 (pWWF98, pWWF83, and pWWF84 [Table 1]). SDS-PAGE showed polypeptides of the expected sizes from all of the pET5a constructs (data not shown).

NagJ, which is homologous to some GSTs, showed no activity in cell extracts of *E. coli*(pWWF51 or pWWF98) against gentisate, maleylpyruvate, or fumarylpyruvate, with or without added GSH. Nor was activity against the same three substrates shown by cell extracts from *E. coli* carrying pWWF71 (*nagMN*), pWWF84 (*nagMN*), pWWF72 (*nagM*), pWWF73 (*nagN*), or pWWF83 (*nagN*).

DISCUSSION

Previous biochemical evidence suggests that there may be more than one route by which gentisate is further metabolized. One metabolic pathway appears to be as we have described in this paper for *Ralstonia* sp. strain U2 and involves the cleavage of the aromatic ring by GDO to form maleylpyruvate, its isomerization to fumarylpyruvate, and subsequent hydrolysis to fumarate and pyruvate. This has been described for a number of different bacteria (5, 8, 24, 26, 27, 41, 49) and was the pathway first elucidated in 1959 by Lack (26). In some bacteria maleylpyruvate isomerization appears to require reduced GSH (8, 27, 41), whereas in the others, particularly gram-positive species, this reaction appears to be GSH independent (8, 18). A third variant of the pathway, in which maleylpyruvate undergoes direct hydrolysis to yield pyruvate and maleate without fumarylpyruvate as an intermediate, has been reported (5, 22). In *P. alcaligenes* P25X1 both a fumarylpyruvate hydrolase and two isofunctional maleylpyruvate hydrolases appear to coexist (5, 39).

Among naphthalene degraders which have been investigated at the genetic level, *Ralstonia* sp. strain U2 appears unique. Within the gene cluster for naphthalene dioxygenase, *nagAa AbAcAd*, there is, between *nagAa* and *nagAb,* an insertion of *nagGH* for salicylate 5-hydroxylase, which converts salicylate to gentisate (14), and downstream of *nagD* is the cluster *nagJI KLMN* described in this paper. The rest of the genes for conversion of naphthalene to salicylate are closely related to the classical upper pathway operon typified by the NAH7 plasmid (9), being homologous and in the same order. A further difference between the *nag* and *nah* clusters is in the regulatory and putative chemotaxis genes *R* and *Y.* In strain U2 both *nagR* and *nagY* are upstream of *nagAa*, whereas in NAH7 both *nahR* (43) and *nahY* (16) are downstream of the upper pathway operon and more closely linked to the *meta*-pathway operon. The similarities between the *nag* and *nah* genes for the conversion of naphthalene to salicylate suggest a common ancestry, but both appear to have independently acquired separate modules of genes for the terminal reactions from salicylate to central metabolites. In NAH7, the genes for salicylate hydroxylase and the *meta*-cleavage pathway are present as a distinct but adjacent operon, whereas in strain U2 genes for the conversion of salicylate through gentisate have been incorporated as part of the same operon by way of an upstream insertion of *nagGH* and a downstream addition of *nagJIKLMN*.

In this paper we have concentrated on elucidating the genetic apparatus for further metabolism of gentisate and have identified the main enzyme components. Our approach was to carry out preliminary experiments, unreported here, to check that the catabolism of gentisate was encoded entirely by the *nagJIKLMN* region and then to clone each gene separately both into pUC18 and into the high-expression vector pET5a. NagI is the GDO converting gentisate to maleylpyruvate, which is then subjected to GSH-dependent isomerization to fumarylpyruvate catalyzed by NagL. We were unable to obtain any evidence that there was a direct hydrolysis of maleylpyruvate to maleate and pyruvate, as has been indicated in other bacteria (5, 22, 39), as none of the *nag* gene products appeared to catalyze this reaction. The hydrolysis of fumarylpyruvate is catalyzed by NagK, and we have demonstrated that pyruvate

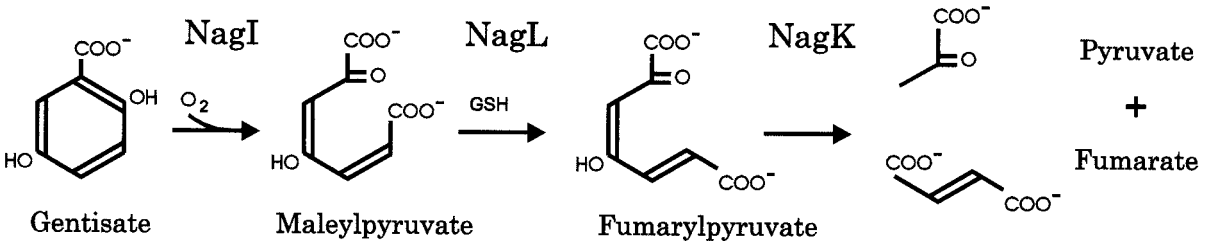

FIG. 6. Reactions of gentisate catabolism catalyzed by the *nag* gene products of *Ralstonia* sp. strain U2.

and fumarate are produced stoichiometrically in this reaction. Together or sequentially, NagI, NagL, and NagK plus added GSH are all that is required to produce pyruvate and fumarate from gentisate in vitro, and it is reasonable to deduce that this is also true in vivo (Fig. 6)

The overall amino acid similarity between NagI and the other complete derived GDO sequences is surprisingly low (35%), perhaps indicating wide divergence within gentisate pathways, possibly as the result of selection for accommodating different substituents on the ring. There is little else in the literature with which to compare the NagL and NagK sequences. One other maleylpyruvate isomerase has been purified, but an N-terminal sequence of only 11 amino acids has been published (41), and only 5 of these are in common with NagL. Although a fumarylpyruvate hydrolase has been purified, no amino acid sequence was determined (5). However, both NagK and NagL show sequence similarities to enzymes with related activities. In both bacteria and eukaryotes the catabolism of phenylalanine and tyrosine proceeds through an analogous pathway in which homogentisate (2,5-dihydroxyphenylacetate) is the ring cleavage substrate and is converted to maleylacetoacetate (11). NagL shows significant similarity to maleylacetoacetate isomerases on this pathway (catalyzing the GSH-dependent conversion to fumarylacetoacetate) in *Sinorhizobium meliloti* (45% identity) (31) and in *Homo sapiens* (41% identity) (12). From Pfam database searches, NagK can be clearly seen to be part of the same family as fumarylacetoacetate hydrolase, which catalyzes the next reaction in the same pathway to produce fumarate and acetoacetate (47).

As has been found in other peripheral catabolic pathways, we have found genes (*nagJ* and *nagMN*) which appear to play no role in the metabolic reactions but which may encode proteins essential to the overall functioning of the pathway in vivo. Interestingly, they each appear to have homologs within the *nag* operon. From database searches NagJ, like NagL, is a member of the GST superfamily, although they are substantially different from each other since the GST family encompasses wide diversity (51). GST-like proteins have been found in other aromatic catabolic pathways (25, 30, 52), of which the most similar to NagJ is BphK (58% identity) in biphenyl catabolism (21). Like NagJ, these have had no function allocated to them. The two other proteins, NagM and NagN, are closer to each other than to any other proteins in the present database and thus constitute another homologous pair: a similar situation has been reported in *C. testosteroni* TA441 (accession no. AB024335), in which there is an adjacent pair of homologous genes (*orf4* and *orf5*) which are also homologous to *nagMN*. The similarity between the NagM and NagN suggested to us that they might encode subunits of a heteromultimeric protein. For this reason, we cloned them in tandem (as well as singly) into both pUC18 and pET5a in case they require coexpression for activity, but we could detect no activity against any of the pathway substrates.

Comparisons with sequences in the databases make it apparent that the gentisate pathway genes we have characterized in strain U2 are present in other bacteria but their functions have not been previously identified. The gene order *nagIKL* corresponds exactly to the homologs *gtdA-orf2-orf3* in *Sphingomonas* sp. strain RW5, which metabolizes 3,6-dichloro-2-methoxybenzoate via gentisate, but the function of only GtdA as a GDO has been demonstrated (53). Based on the gene order and protein similarity between the genes in these two clusters, we predict that the enzymes encoded by *orf2* and *orf3* in strain RW5 are a fumarylpyruvate hydrolase and a GSH-dependent maleylpyruvate isomerase, respectively. If this is correct, the metabolism of maleylpyruvate in RW5 is also via a GSH-dependent isomerization to fumarylpyruvate and then to fumarate and pyruvate by hydrolysis. A similar situation may well apply to *Sphingomonas* sp. strain RW1, where two adjacent ORFs corresponding to *nagKL* have been reported (3). In *K. pneumoniae*, a similar gene order was deduced but without sequence determination: this was *mhbD* (for GDO), *mhbH* (for fumarylpyruvate hydrolase), and *mhbI* (for GSH-dependent maleylpyruvate isomerase isomerase) but with the difference of the insertion of *mhbM* (for 3-hydroxybenzoate monooxygenase, catalyzing the conversion of 3-hydroxybenzoate to gentisate), between *mhbH* and *mhbI* (41).

ACKNOWLEDGMENTS

We thank Linda Shaw for technical help particularly with the sequence determination.

This research was supported by the Biotechnology and Biological Sciences Research Council. S.L.F. was jointly funded by a visiting fellowship from the Royal Society and the National Council for Scientific and Technological Research (CONICIT), Venezuela.

REFERENCES

1. **Altschul, S. F., W. Gish, W. Miller, E. W. Myers, and D. J. Lipman.** 1990. Basic local alignment search tool. J. Mol. Biol. **215:**403–410.
2. **Arai, H., T. Yamamoto, T. Ohishi, T. Shimizu, T. Nakata, and T. Kudo.** 1999. Genetic organization and characteristics of the 3-(3-hydroxyphenyl)propionic acid degradation pathway of *Comamonas testosteroni* TA441. Microbiology (United Kingdom) **145:**2813–2820.
3. **Armengaud, J., and K. N. Timmis.** 1997. Molecular characterization of Fdx1, a putidaredoxin-type [2Fe-2S] ferredoxin able to transfer electrons to the dioxin dioxygenase of *Sphingomonas* sp. RW1. Eur. J. Biochem. **247:**833–842.
4. **Bateman, A., E. Birney, R. Durbin, S. R. Eddy, K. L. Howe, and E. L. L. Sonnhammer.** 2000. The Pfam protein families database. Nucleic Acids Res. **28:**263–266.
5. **Bayly, R., P. Chapman, S. Dagley, and D. Di Berardino.** 1980. Purification and some properties of maleylpyruvate hydrolase and fumarylpyruvate hydrolase from *Pseudomonas alcaligenes*. J. Bacteriol. **143:**70–77.

6. **Cane, P. A., and P. A. Williams.** 1986. A restriction map of naphthalene catabolic plasmid pWW60–1 and the location of some of its catabolic genes. J. Gen. Microbiol. **132:**2919–2929.
7. **Crawford, R., S. Hutton, and P. Chapman.** 1975. Purification and properties of gentisate 1,2-dioxygenase from *Moraxella osloensis*. J. Bacteriol. **121:**794–799.
8. **Crawford, R. L., and T. D. Frick.** 1977. Rapid spectrophotometric differentiation between glutathione-dependent and glutathione-independent gentisate and homogentisate pathways. Appl. Environ. Microbiol. **34:**170–174.
9. **Eaton, R. W.** 1994. Organization and evolution of naphthalene catabolic pathways: sequence of the DNA encoding 2-hydroxychromene-2-carboxylate isomerase and *trans-o*-hydroxybenzylidenepyruvate hydratase-aldolase from the NAH7 plasmid. J. Bacteriol. **176:**7757–7762.
10. **Feng, Y. M., H. E. Khoo, and C. L. Poh.** 1999. Purification and characterization of gentisate 1,2-dioxygenases from *Pseudomonas alcaligenes* NCIB 9867 and *Pseudomonas putida* NCIB 9869. Appl. Environ. Microbiol. **65:** 946–950.
11. **Fernandez-Canon, J. M., and M. A. Penalva.** 1995. Molecular characterization of a gene encoding a homogentisate dioxygenase from *Aspergillus nidulans* and identification of its human and plant homologs. J. Biol. Chem. **270:**21199–21205.
12. **Fernandez-Canon, J. M., and M. A. Penalva.** 1998. Characterization of a fungal maleylacetoacetate isomerase gene and identification of its human homologue. J. Biol. Chem. **273:**329–337.
13. **Fu, W. J., and P. Oriel.** 1998. Gentisate 1,2-dioxygenase from *Haloferax* sp. D1227. Extremophiles **2:**439–446.
14. **Fuenmayor, S. L., M. Wild, A. L. Boyes, and P. A. Williams.** 1998. A gene cluster encoding steps in conversion of naphthalene to gentisate in *Pseudomonas* sp. strain U2. J. Bacteriol. **180:**2522–2530.
15. **Goetz, F. E., and L. J. Harmuth.** 1992. Gentisate pathway in *Salmonella typhimurium*: metabolism of *m*-hydroxybenzoate and gentisate. FEMS Microbiol. Lett. **97:**45–49.
16. **Grimm, A. C., and C. S. Harwood.** 1999. NahY, a catabolic plasmid-encoded receptor required for chemotaxis of *Pseudomonas putida* to the aromatic hydrocarbon naphthalene. J. Bacteriol. **181:**3310–3316.
17. **Grund, E., B. Denecke, and R. Eichenlaub.** 1992. Naphthalene degradation via salicylate and gentisate by *Rhodococcus* sp strain B4. Appl. Environ. Microbiol. **58:**1874–1877.
18. **Hagedorn, S. R., G. Bradley, and P. J. Chapman.** 1985. Glutathione-independent isomerization of maleylpyruvate by *Bacillus megaterium* and other gram-positive bacteria. J. Bacteriol. **163:**640–647.
19. **Harpel, R. M., and J. D. Lipscomb.** 1990. Gentisate 1,2-dioxygenase from *Pseudomonas*. Substrate coordination to active site Fe^{2+} and mechanism of turnover. J. Biol. Chem. **265:**22187–22196.
20. **Harpel, R. M., and J. D. Lipscomb.** 1990. Gentisate 1,2-dioxygenase from *Pseudomonas*—purification, characterization, and comparison of the enzymes from *Pseudomonas testosteroni* and *Pseudomonas acidovorans*. J. Biol. Chem. **265:**6301–6311.
21. **Hofer, B., S. Backhaus, and K. N. Timmis.** 1994. The biphenyl polychlorinated biphenyl-degradation locus (*bph*) of *Pseudomonas* sp LB400 encodes 4 additional metabolic enzymes. Gene **144:**9–16.
22. **Hopper, D. J., P. J. Chapman, and S. Dagley.** 1968. Enzymic formation of D-malate. Biochem. J. **110:**798–800.
23. **Jain, R. K.** 1996. The molecular cloning of genes specifying some enzymes of the 3,5-xylenol degradative pathway. Appl. Microbiol. Biotechnol. **45:**502–508.
24. **Jones, D. C. N., and R. A. Cooper.** 1990. Catabolism of 3-hydroxybenzoate by the gentisate pathway in *Klebsiella pneumoniae* M5a1. Arch. Microbiol. **154:** 489–495.
25. **Kimura, N., A. Nishi, M. Goto, and K. Furukawa.** 1997. Functional analyses of a variety of chimeric dioxygenases constructed from two biphenyl dioxygenases that are similar structurally but different functionally. J. Bacteriol. **179:**3936–3943.
26. **Lack, L.** 1959. The enzymic oxidation of gentisic acid. Biochim. Biophys. Acta **34:**117–123.
27. **Lack, L.** 1961. Enzymic *cis-trans* isomerisation of maleylpyruvic acid. J. Biol. Chem. **236:**2835–2840.
28. **Lane, D. J.** 1991. 16S/23S rRNA sequencing, p. 115–148. *In* E. Stackebrandt and M. Goodfellow (ed.), Nucleic acid techniques in bacterial systematics. John Wiley and Sons, New York, N.Y.
29. **Lian, H. L., and C. P. Whitman.** 1993. Ketonization of 2-hydroxy-2,4-pentadienoate by 4-oxalocrotonate tautomerase—implications for the stereochemical course and the mechanism. J. Am. Chem. Soc. **115:**7978–7984.
30. **Lloyd-Jones, G., and P. C. K. Lau.** 1997. Glutathione *S*-transferase-encoding gene as a potential probe for environmental bacterial isolates capable of degrading polycyclic aromatic hydrocarbons. Appl. Environ. Microbiol. **63:** 3286–3290.
31. **Milcamps, A., and F. J. de Bruijn.** 1999. Identification of a novel nutrient-deprivation-induced *Sinorhizobium meliloti* gene (*hmgA*) involved in the degradation of tyrosine. Microbiology (United Kingdom) **145:**935–947.
32. **Miller, J. H.** 1972. Experiments in molecular genetics. Cold Spring Harbor Laboratory Press, Cold Spring Harbor, N.Y.
33. **Moissenet, D., C. P. Goujon, A. Garbarg-Chenon, and H. Vu-Thien.** 1999. CDC group IV c-2: a new *Ralstonia* species close to *Ralstonia eutropha*. J. Clin. Microbiol. **37:**1777–1781.
34. **Monticello, D. J., D. Bakker, M. Schell, and W. R. Finnerty.** 1985. Plasmid-borne Tn*5* insertion mutation resulting in accumulation of gentisate from salicylate. Appl. Environ. Microbiol. **49:**761–764.
35. **Mutoh, N., and M. I. Simon.** 1986. Nucleotide sequence corresponding to five chemotaxis genes in *Escherichia coli*. J. Bacteriol. **165:**161–166.
36. **Nakatsu, C., J. Ng, R. Singh, N. Straus, and C. Wyndham.** 1991. Chlorobenzoate catabolic transposon Tn5271 is a composite class-I element with flanking class-II insertion sequences. Proc. Natl. Acad. Sci. USA **88:**8312–8316.
37. **Ohmoto, T., K. Sakai, N. Hamada, and T. Ohe.** 1991. Salicylic acid metabolism through a gentisate pathway by *Pseudomonas* sp TA-2. Agri. Biol. Chem. **55:**1733–1737.
38. **Osterhout, G. J., J. L. Valentine, and J. D. Dick.** 1998. Phenotypic and genotypic characterization of clinical strains of CDC group IVc-2. J. Clin. Microbiol. **36:**2618–2622.
39. **Poh, C. L., and R. Bayly.** 1980. Evidence for isofunctional enzymes used in *m*-cresol and 2,5-xylenol degradation via gentisate pathway in *Pseudomonas alcaligenes*. J. Bacteriol. **143:**59–69.
40. **Rani, M., D. Prakash, R. C. Sobti, and R. K. Jain.** 1996. Plasmid-mediated degradation of *o*-phthalate and salicylate by a *Moraxella* sp. Biochem. Biophys. Res. Commun. **220:**377–381.
41. **Robson, N. D., S. Parrott, and R. A. Cooper.** 1996. *In vitro* formation of a catabolic plasmid carrying *Klebsiella pneumoniae* DNA that allows growth of *Escherichia coli* K-12 on 3-hydroxybenzoate. Microbiology (United Kingdom) **142:**2115–2120.
42. **Sambrook, J., E. F. Fritsch, and T. Maniatis (ed.).** 1989. Molecular cloning: a laboratory manual, 2nd ed. Cold Spring Harbor Laboratory Press, Cold Spring Harbor, N.Y.
43. **Schell, M. A.** 1986. Homology between nucleotide sequences of promoter regions of *nah* and s*al* operons of NAH7 plasmid of *Pseudomonas putida*. Proc. Natl. Acad. Sci. USA **83:**369–373.
44. **Schell, A. M., and M. Sukordhaman.** 1989. Evidence that the transcription activator encoded by the *Pseudomonas putida nahR* gene is evolutionarily related to the transcription activators encoded by the *Rhizobium nodD* genes. J. Bacteriol. **171:**1952–1959.
45. **Simon, J. M., T. D. Osslund, R. Saunders, B. D. Ensley, S. Suggs, A. Harcourt, W. C. Suen, D. L. Cruden, D. T. Gibson, and G. J. Zylstra.** 1993. Sequences of genes encoding naphthalene dioxygenase in *Pseudomonas putida* strains G7 and NCIB 9816-4. Gene **127:**31–37.
46. **Southern, E. M.** 1975. Detection of specific sequences among DNA fragments separated by gel electrophoresis. J. Mol. Biol. **98:**503–517.
47. **St Louis, M., and R. M. Tanguay.** 1997. Mutations in the fumarylacetoacetate hydrolase gene causing hereditary tyrosinemia type I: overview. Hum. Mutat. **9:**291–299.
48. **Studier, F. W., and B. A. Moffatt.** 1986. Use of bacteriophage T7 RNA polymerase to direct selective high level expression of cloned genes. J. Mol. Biol. **189:**113–130.
49. **Tanaka, H., S. Sugiyama, K. Yano, and K. Arima.** 1957. Isolation of fumarylpyruvic acid as an intermediate of the gentisic acid oxidation by *Pseudomonas ovalis* var. S-5. Agr. Chem. Soc. Jpn. Bull. **21:**67–68.
50. **van Damme, P., J. Goris, T. Coenye, B. Hoste, D. Janssens, K. Kersters, P. de Vos, and E. Falsen.** 1999. Assignment of centers for disease control group IVc-2 to the genus *Ralstonia* as *Ralstonia paucula* sp. nov. Int. J. Syst. Bacteriol. **49:**663–669.
51. **Vuilleumier, S.** 1997. Bacterial glutathione *S*-transferases: what are they good for? J. Bacteriol. **179:**1431–1441.
52. **Wang, Y., P. C. K. Lau, and D. K. Button.** 1996. A marine oligobacterium harboring genes known to be part of aromatic hydrocarbon degradation pathways of soil pseudomonads. Appl. Environ. Microbiol. **62:**2169–2173.
53. **Werwath, J., H. A. Arfmann, D. H. Pieper, K. N. Timmis, and R. M. Wittich.** 1998. Biochemical and genetic characterization of a gentisate 1,2-dioxygenase from *Sphingomonas* sp. strain RW5. J. Bacteriol. **180:**4171–4176.
54. **Wheatcroft, R., and P. A. Williams.** 1981. Rapid methods for the study of both stable and unstable plasmids in *Pseudomonas*. J. Gen. Microbiol. **124:** 433–437.
55. **Williams, P. A., and B. N. Zaba.** 1997. EnzPack for Windows. Biosoft, Cambridge, United Kingdom.
56. **Worsey, M. J., and P. A. Williams.** 1975. Metabolism of toluene and xylenes by *Pseudomonas putida* (*arvilla*) mt-2: evidence for a new function of the TOL plasmid. J. Bacteriol. **124:**7–13.
57. **Yanisch-Perron, C., J. Vieira, and J. Messing.** 1985. Improved M13 phage cloning vectors and host strains: nucleotide sequences of the M13mp18 and pUC19 vectors. Gene **33:**103–119.